JET AND MISSING TRANSVERSE ENERGY AT THE LHC *

Martine Bosman
Institut de Física d'Altes Energies, IFAE-UAB Barcelona
For the ATLAS and CMS Collaborations

Abstract

Many physics channels of interest at the LHC involve the measurement of jets and missing transverse momentum. The various physics and detector effects playing a role in the chain that goes from an initial parton produced in the hard scattering process to a reconstructed and calibrated jet in the calorimeters are reviewed. The most relevant issues for a good performance in missing transverse momentum measurement are described. The expected performances of the ATLAS and CMS detectors are presented for some of the characteristics physics channels at the LHC. Jet and E_T^{miss} triggers are discussed.

ATL-CONF-2002-001
21/01/2002

1 Introduction

Various roles will be played by jets in the LHC Physics. The measurement of jet multiplicity and E_T distribution will be done in the context of QCD, SUSY or other models. Resonances will be identified by their decay to jets like $W \to jj$, $t \to bW$, $Z \to b\overline{b}$, $Z' \to jj$. Central low p_T jet veto will be applied to eliminate multi-jet background like $t\overline{t}$. Forward jets will be tagged to select boson fusion mechanisms. Large E_T^{miss} will be an important signature for new physics. The p_T^{miss} vector will be used in invariant mass reconstruction of decays involving neutrinos like $A/H \to \tau\overline{\tau}$ decays.

2 ATLAS and CMS calorimetry

The requirements set on the calorimetry to achieve the physics goals at the LHC are listed hereafter. The pseudorapidity (η) coverage should extend to $\mid \eta \mid \simeq 5$ for good E_T^{miss} resolution and forward jet tagging capability. The

*Talk presented at the IX Int. Conf. on Calorimetry in Particle Physics - Annecy, Oct. 9-14, 2000

detector should be hermetic: the necessary gaps for services should not form uninstrumented "cracks" pointing to the interaction region in order to avoid tails from badly reconstructed jets. The calorimeter thickness should reach at least ~ 9 interaction lengths (λ) to avoid longitudinal leakage of high energy pions and reduce punch-through in the muon detector. The granularity is adapted to the lateral hadronic shower size: $d\eta \times d\phi = 0.087 \times 0.087$ in the case of CMS and $d\eta \times d\phi = 0.1 \times 0.1$ for ATLAS. The calorimeters are composed of the electromagnetic (EM) calorimeter followed by an hadronic (HAD) compartment with optimized longitudinal segmentation (see fig.1). In case of ATLAS[1], the EM calorimeter

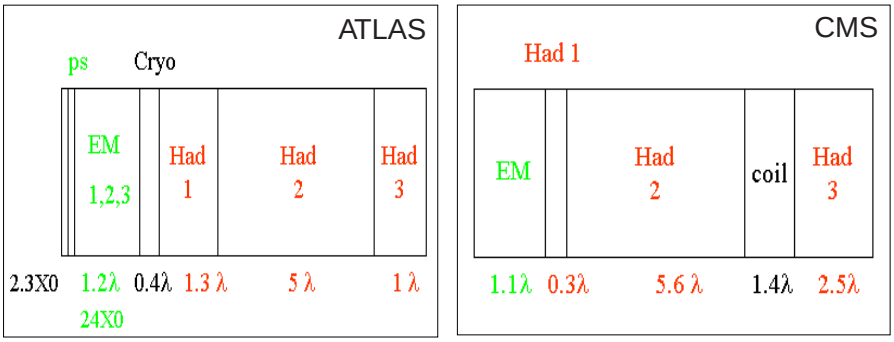

Figure 1: *Schematic representation of the longitudinal segmentation of the ATLAS and CMS barrel sections of the calorimeter.*

consists of 24 radiation lengths (X_0) or 1.2 λ of Pb/LAr calorimeter with three longitudinal sections for (γ, jet) separation. The EM calorimeter is preceded by a preshower to correct for the energy loss in the solenoid coil and cryostat wall situated just in front of the calorimeter. The outer cryostat wall (0.4λ) separates the EM from the Fe/Scintillating Tile hadron calorimeter. In the end-cap region ($\sim 1.7 <| \eta |<\sim 3$) Cu/LAr technology is used. While the forward region, covering $\sim 3 <| \eta |<\sim 5$, consists of a Cu/LAr EM section followed by a W/LAr section. In CMS[2], the PbW04 crystal EM calorimeter ($\sim 1.1\lambda$) is combined with a Cu/Scintillating Tile calorimeter, both in the barrel and end-cap region. The latter is segmented in a thin section (0.3λ) followed by the bulk of the calorimeter (5.6 λ). It is surrounded by the solenoid coil (1.4λ). Two instrumented layers in the muon system provide an additional 2.5λ of active calorimeter. The forward region is equipped with a Fe calorimeter instrumented with quartz fibers.

Both CMS and ATLAS calorimeters are non-compensated. The degree of non-compensation of the CMS hadronic section is $e/h \simeq 1.4$ while for ATLAS

the degree is $e/h \simeq 1.35$. The degree of non-compensation of the EM section is substantially higher in both cases. This results in a non-linearity of the pion response of about 15% between 20 and 300 GeV for CMS and about 12% for ATLAS. The resolution and linearity depend on the algorithm used for energy reconstruction. CMS used a simple sum $E_{tot} = E_{EM} + (\alpha \times H_1 + H_2 + H_3)$. A large signal in H_1 indicates that a significant amount of hadronic energy was deposited in the EM, the coefficient α corrects for the fact that this energy is underestimated because of non-compensation. The resolution is $\sigma_E/E = 122\%/\sqrt{(E)} \oplus 5\%$. ATLAS used in the test beam an algorithm that includes a first order correction for non-compensation (quadratic term in E_{EM}) and an interpolation term between the last EM section (E_{EM3}) and the first hadronic section (E_{HAD1}) to estimate the energy loss in the cryostat: $E_{tot} = \alpha \times E_{EM} + \beta \times E_{EM}^2 + \gamma \times E_{HAD} + \delta \times \sqrt{E_{EM3} \times E_{HAD1}}$. The resolution is $\sigma_E/E = 50\%/\sqrt{E} \oplus 3.4\% \oplus 1.0/E$ applying a 2σ noise cut and reconstructing the pion energy in a cone of $dR = 0.3$.

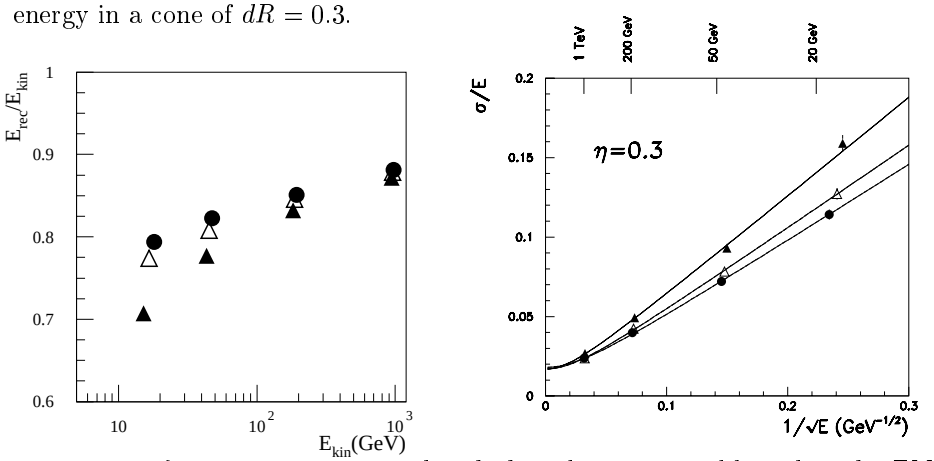

Figure 2: *Left: jet energy measured with the calorimeters calibrated at the EM scale in cone sizes of dR=1.5 (black circles), dR=0.7 (open triangles), dR=0.4 (black triangles); Right: jet energy resolution at $\eta = 0.3$ for various cone sizes after applying a jet energy calibration algorithm (ATLAS).*

3 Jet Reconstruction

There are various factors that play a role in the chain between the initial parton and the reconstructed jet. Among the experimental factors are the different response to neutral and charged component (non-linearity), the lateral shower size, dead material and cracks, longitudinal leakage, and magnetic field. The factors related to physics are fragmentation, initial state radiation, final state radiation, underlying event and minimum bias events.

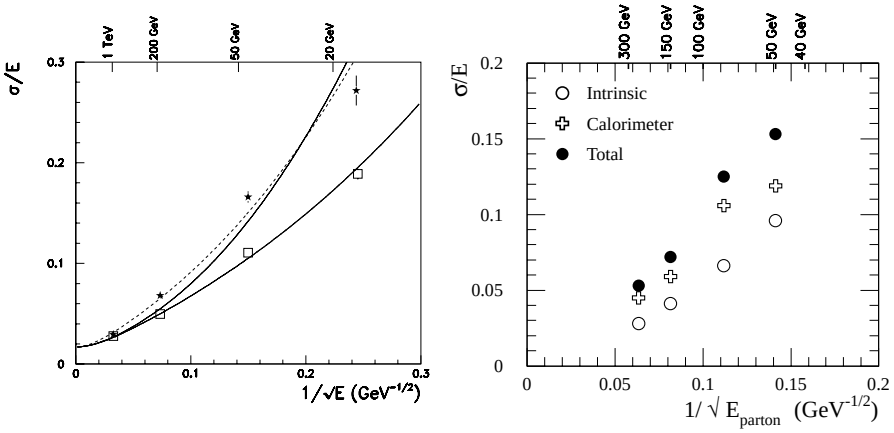

Figure 3: *Left: jet energy resolution (calorimeter contribution) without pile-up (open squares) and with high-luminosity pile-up events (stars) for a cone size of dR=0.4. Right: the intrinsic physics contribution to the resolution (open circles) and the calorimeter related resolution (open crosses); combined in quadrature (black dots) they represent the resolution with which the parton energy is measured.*

The ratio of reconstructed jet energy to the particle level energy inside the cone, when the calorimeters are calibrated at the EM scale, is typically of the order of 0.8 (see fig.2 left). It increases with jet energy, as the pions from the fragmentation get more energetic, and decreases for smaller cone size due to lateral shower containment effects. The jet energy reconstruction algorithm has to correct for these effects. The calorimeter contribution to the jet energy resolution, measured in ATLAS using the particle level energy as a reference, is shown in fig.2 at $\eta = 0.3$. The jet calibration algorithm included energy dependent weights for the different calorimeter compartments and correction terms for energy loss in dead materials. The resolution is $\sigma_E/E = 48\%/\sqrt{E} \oplus 1.7\%$ for a very large cone (dR=1.5). The sampling term increases to 52% (62%) for a cone size of dR=0.7 (dR=0.4) due to the fluctuations of out of cone losses for low energy jets. For high energy jets the particles are very collimated and do not suffer from these losses. But for larger η, the pseudorapidity lines become progressively denser, hence out-of-cone losses start to affect also high energy jets, resulting in an increase of the constant term for small cone sizes.

The electronic noise is another detector related effect that influences the resolution. In ATLAS, the level of noise is 200 MeV in a tower $d\eta \times d\phi = 0.1 \times 0.1$ and 0.7 GeV (1.4 GeV) in a cone of dR=0.4 (0.7). In CMS, the level is 150 MeV in a tower of $d\eta \times d\phi = 0.087 \times 0.087$. Once the jet energy calibration is applied,

the electronic noise contributes a 1.7 GeV/E term to the jet energy resolution for a dR=0.4 cone. At high luminosity, minimum bias events generate 0.5 GeV of transverse energy in a tower $d\eta \times d\phi = 0.1 \times 0.1$ and 3.5 GeV (14 GeV) in a cone of radial aperture dR=0.4 (0.7) (el. noise included). Minimum bias deteriorates notably the resolution of low E_T jets (see fig 3 left). The resolution becomes $\sigma_E/E = 62\%/\sqrt{E} \oplus 1.5\% \oplus 4.7/E$. Large cones like dR=0.7 cannot be used at high luminosity.

In the chain that goes from the parton to a reconstructed jet in a "cone", physics related effects also contribute to the resolution: fluctuation in the fragmentations, FSR, underlying events, magnetic field sweeping particles out of the cone (p_T cutoff of 0.5 GeV ATLAS and 0.9 GeV in CMS). This "intrinsic" contribution is shown in fig.3 together with the calorimeter contribution for a fixed cone algorithm (dR=0.4) applied to $Z^0 + jet$ events.

4 Jet Algorithms

There are two basic approaches but many possible variations. In "cone-like" algorithms a cone is drawn around a seed. There are variant on how the cone direction is iterated, how jet overlap is handled, etc. "Clustering" algorithms (QCD inspired) pair "particles" (approximated by calorimeter towers) starting from the "closest" particles. They stop at a fixed jet multiplicity or a maximum "size", etc. The various algorithms suffer from different energy bias as a function of E_T originating from physics effect like pile-up (luminosity dependent) or experimental effects like detector non-linearity and shower size effects. These effects depend on jet particle composition and reconstructed size. The choice of jet algorithm will depend on the physics channel and luminosity conditions. For example, different algorithms will be used for QCD jet multiplicity study at low luminosity or for high p_T $W \to jj$ reconstruction at high luminosity. The jet energy calibration will be a complex issue because of the combination of physics and detector effects that depend on the jet algorithm and the luminosity. In-situ physics processes like $Z^0 + jet$ and $W \to jj$ will be used, combined with test beam information.

5 Reconstruction of resonances

Reconstruction of resonances decaying to jets will be used in many physics analysis. $W \to jj$ decays are of interest in a wide range of p_T of the W. An example of jj invariant mass reconstructed with ATLAS at low luminosity is given in the fig.4 (left) for W with p_T in the range 120-150 GeV. The resolution

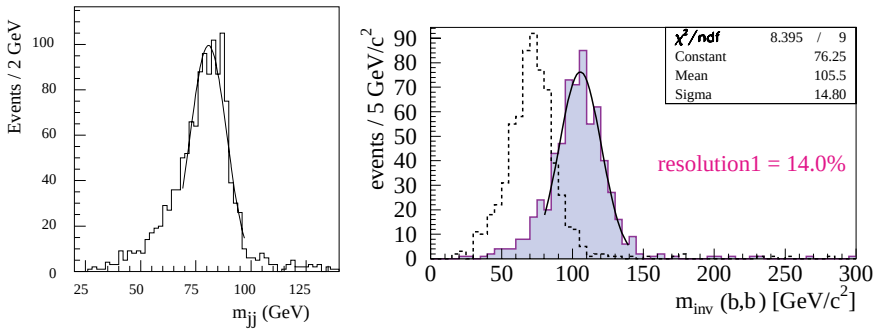

Figure 4: *Left:* $\sim$ 150 GeV p_T $W \to jj$ *decays reconstructed in ATLAS at low luminosity. Right:* $H \to b\overline{b}$ *decay at high luminosity reconstructed in CMS before calibration (dotted line) and after calibration (shaded area).*

is $\sim 8\ GeV$; it increases to $\sim 13\ GeV$ at high luminosity. The tail at low mass is due to a bias in the jet direction when the jets overlap, a feature that gets more pronounced with the boost due of a high p_T decaying object. An example of a 110 GeV Higgs decaying to $b\overline{b}$ as reconstructed at high luminosity with the CMS detector is shown in fig.4 (right). The resolution is $\sim 14\ GeV$ at high luminosity.

6 Jet trigger

The jet cross-section is very steeply falling with p_T: $d\sigma/dp_T \sim 1/p_T^3$. The sharpness of the efficiency curve is important to avoid that the trigger rate is dominated by lower p_T jets. At the Level-1 trigger, both ATLAS and CMS use a sliding window algorithm searching for a local maximum in the $(d\eta \times d\phi)$ projected transverse energy map. The optimum window size depends on the jet E_T threshold and the luminosity conditions (programmable in the case of ATLAS). CMS applies a two-parameter η dependent energy correction algorithm that improves the resolution and consequently the sharpness of the efficiency curve as shown in fig.5 (left). At Level-2 or Level-3, standard offline jet algorithms can be applied with a better jet energy calibration. A reduction of rate of about a factor two is seen in ATLAS with respect to the Level-1 rate. If the allocated bandwidth for jet triggers is set for example to 25 Hz, then the corresponding E_T thresholds to be applied are 360 GeV, 150 GeV, 100 GeV for single-, three-, four-jet triggers respectively at low luminosity.

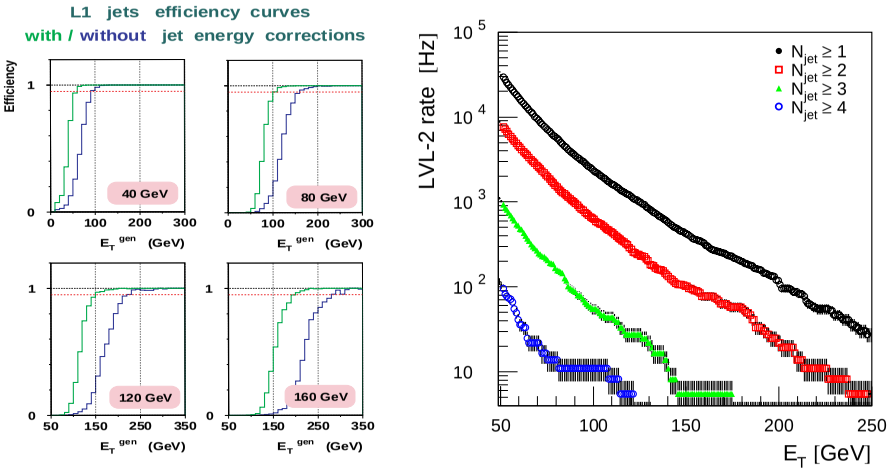

Figure 5: *Left: CMS Level-1 trigger efficiency curves for various thresholds with and without jet energy corrections; Right: ATLAS Level-2 trigger rates for various jet multiplicities at low luminosity.*

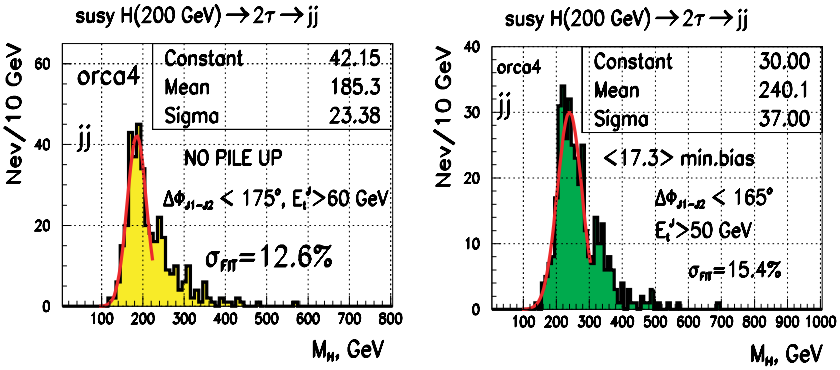

Figure 6: *200 GeV $A/H \to \tau\tau \to jj$ decays reconstructed at low luminosity (left) and high luminosity (right) with the CMS detector.*

7 τ jets

τ jets are narrow, isolated jets associated to 1(3) track(s). On the base of these characteristics, they are separated from QCD jets (these criteria can also be applied at trigger level). For example, ATLAS can reach in the offline reconstruction a factor of ~ 100 QCD jet rejection for a τ efficiency of $\sim 50\%$. The invariant mass of resonances decaying to τ jets can be reconstructed from the τ visible decay products and the p_T^{miss} vector as a measure of the neutrino component. One interesting example is the $A/H \to \tau\tau$ decay. Fig.6 shows $A/H \to \tau\tau \to jj$ decays reconstructed with the CMS detector at low and high luminosity.

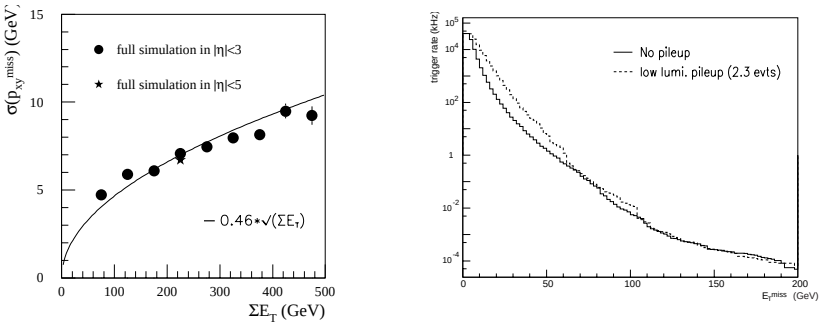

Figure 7: *Left: resolution of the two components of the E_T^{miss} vector as a function of the total transverse energy in the calorimeters at low luminosity. Right: inclusive E_T^{miss} trigger rates from QCD jet events as a function of the E_T^{miss} threshold applied at Level-1.*

8 E_T^{miss} reconstruction

The p_T^{miss} vector is used for invariant mass reconstruction like the $A/H \to \tau\tau$ decay, henceforth a good resolution is important. Large E_T^{miss} will be an important signature for new physics like for example in SUSY models. Tails from fake E_T^{miss} due to instrumental effects like "cracks", generating tails in the reconstructed jet energy, have to be minimized. The p_T^{miss} vector is reconstructed from cell (or tower) energies. The important factors for the resolution as studied by ATLAS with $A/H \to \tau\tau$ decays are the following. A calorimeter coverage up to $\mid \eta \mid \sim 5$ is needed. The resolution $\sigma(p_{X,Y}^{miss})$, measured at particle level, increases from 2.3 GeV to 8.3 GeV if the coverage decreases from $\mid \eta \mid \sim 5$ to $\mid \eta \mid \sim 3$. The particle level resolution $\sigma(p_{X,Y}^{miss})$ increases to 7 GeV when the detector response is fully simulated. The contribution to the calorimeter resolution depends on $\mid \eta \mid$. The contribution from the different regions are: barrel (5 GeV), end cap (4 GeV), forward (3 GeV) decreasing because the average transverse energy in the various regions decreases. The electronic noise (a 1.5 σ cut is applied) increases the resolution from 8.3 GeV to 9 GeV. The $p_{X,Y}^{miss}$ resolution can be parameterized as $\sigma(p_{X,Y}^{miss}) = 0.46 \times \sqrt{\Sigma E_T}$ (see fig.7). At high luminosity, the pile-up events contribute an additional 15 GeV to the resolution. At the Level-1 trigger the E_T^{miss} is calculated from tower E_T with a granularity of $d\eta \times d\phi = 0.348 \times 0.348$ in CMS and 0.2×0.2 in ATLAS. In both cases the least significant bit is 1 GeV. At Level-3, E_T^{miss} can be recalculated with finer granularity and better calibration constants. The Level-1 rate is dominated by QCD Dijet events and pile-up. An ATLAS estimate of the trigger rate at low luminosity is shown in fig.7. Below 60 GeV, minimum bias events increase the

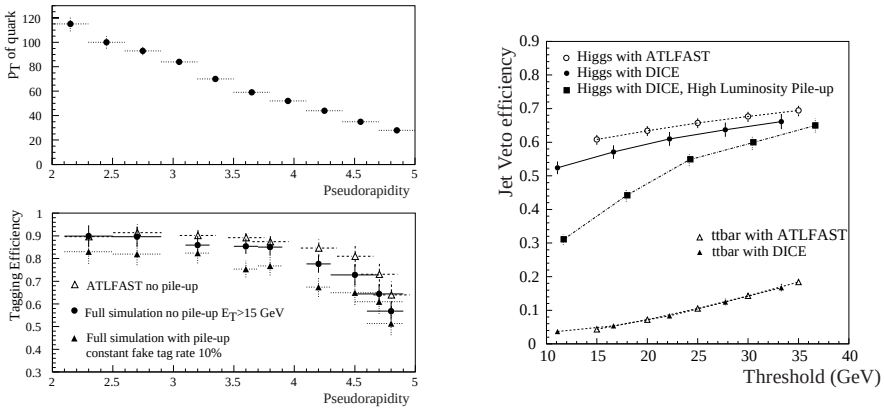

Figure 8: *Left: Average p_T of forward quarks and forward jet tagging efficiency in ATLAS at low and high luminosity. Right: Jet veto efficiency for heavy Higgs an $t\bar{t}$ events for fast simulation and full simulation (DICE) in ATLAS.*

rate by a factor ~ 5; above 100 GeV the pile-up has no effect anymore. At high luminosity, the rates increase by a factor $\sim 10^3$ for a 100 GeV threshold and ~ 10 for a 200 GeV threshold.

9 Forward jet tagging and low p_T jet veto

Forward jet tagging will be used to select boson fusion processes (see fig.8 left). A tagging efficiency of $\sim 90\%$ can be achieved starting to decrease at $\mid \eta \mid \geq 4$ because of the decreasing average p_T of the quark. At high luminosity, an efficiency of $\sim 80\%$ can be achieved for a fake tag rate of $\sim 10\%$. Central jet veto is used to reject high jet multiplicity background, usually $t\bar{t}$. Fig.8 shows that in ATLAS an efficiency of $\sim 60\%$ is achieved for a heavy $H \rightarrow WW \rightarrow l\nu jj$ signal and $\sim 10\%$ for the $t\bar{t}$ background.

10 Conclusion

There is a lot of interesting physics involving jets and E_T^{miss} at the LHC. The ATLAS and CMS detectors have shown that their calorimeters are prepared to trigger and reconstruct these quantities in the challenging environment of a high luminosity hadron collider.

11 Acknowledgement

The author would like to thank S.Arcelli, S.Abdullin, ... from CMS, C.Santoni and many more colleagues from ATLAS for material and useful discussions.

References

[1] The ATLAS calorimeter Performance Technical Design Report, CERN/LHCC 96-40.

[2] The CMS Hadron Calorimeter Project Technical Design Report, CERN/LHCC 97-31.

[3] The ATLAS Detector and Physics Performance Technical Design Report, CERN/LHCC 99-14.

[4] Studies of the response of the prototype CMS Hadron calorimeter, including magnetic field effects to pion, electron and muon beams. V.V. Abramov et al.,hep-ex/0007045,Jul. 2000